# Radiative muon absorption in oxygen

A. Frischknecht,* M. Döbeli,† W. Stehling,‡ G. Strassner,§ and P. Truöl
*Physik Institut der Universität Zürich, 8001 Zürich, Switzerland*

J. C. Alder,** C. Joseph, J. F. Loude, J. P. Perroud, D. Ruegger, and M. T. Tran
*Institut de Physique Nucléaire, Université de Lausanne, 1015 Lausanne, Switzerland*

H. Panke††
*Sektion Physik, Universität München, 8046 Garching, Germany*
(Received 20 May 1988)

The photon spectrum from radiative absorption of negative muons in $^{16}O$ has been measured with a high-resolution pair spectrometer. The integrated branching ratio for photons with energies greater than 57 MeV relative to the total muon absorption rate is $(3.8\pm0.4)\times10^{-5}$. The data are consistent with nuclear model calculations for a value of the induced pseudoscalar coupling in $^{16}O$ of $g_P/g_A=13.5\pm1.5$.

## I. INTRODUCTION

We have recently reported the results of an experiment[1] in which we measured the photon spectra and integrated rates for radiative muon absorption in various nuclei, ranging from $^{12}C$ to $^{209}Bi$. From the comparison of this data with nuclear model calculations,[2] some insight could be gained on the evolution of the induced pseudoscalar coupling of the semileptonic weak interaction in a nuclear environment. For the lightest systems studied the values extracted for the induced pseudoscalar coupling constant $g_P$ slightly exceed the nucleonic value $g_P=(7.0\pm1.5)g_A$,[3] but are still consistent with it within the large error bars. For the medium-heavy system $^{40}Ca$ a 50% quenching is observed, while the heavier target data indicate a complete absence of this coupling. In this experiment we used a double-arm total absorption NaI spectrometer with moderate photon energy resoluation ($\Delta E/E\approx15\%$ FWHM) and reasonable acceptance ($\Delta\Omega/4\pi\approx4\times10^{-3}$) rendered neutron insensitive by photon conversion and subsequent identification of the electron-positron pairs with a threshold Čerenkov counter.

Prior to these data, experiments[2] had concentrated on $^{40}Ca$. For this nucleus our data agree well with data of a previous experiment[4] employing a technique similar to ours and more precise older data of our own group.[5] In this latter experiment photons were detected in a high-resolution magnetic pair spectrometer ($\Delta E/E\approx1.5\%$) with a low acceptance ($\Delta\Omega/4\pi\approx6\times10^{-5}$) but inherently insensitive to the copious neutron background in muon absorption. We emphasize the difference between the experimental tools, since it is in particular the neutron background, which, combined with the low radiative branching ratio made this type of experiment notoriously difficult and led to quite a few conflicting early results.[2]

In this paper we address a remaining discrepancy concerning the radiative muon capture branching ratio in $^{16}O$. Preliminary analysis of data from our pair spectrometer run[6] and the final analysis of the data from the NaI spectrometer run[1] gave conflicting results,

$$B_\gamma=\Lambda(\mu^-,\nu_\mu\gamma;E_\gamma>57\ \text{MeV}/\Lambda(\mu^-,\text{all})$$
$$=(6.2\pm0.8)\times10^{-5}\ ,$$

and

$$B_\gamma=(2.5\pm0.5)\times10^{-5}$$

(Refs. 6 and 1, respectively). The pair spectrometer calibration data taken for the $^{40}Ca$ experiment[5] allowed also a final evaluation of the $^{16}O(\mu^-,\nu_\mu\gamma)^{16}N$ spectra taken with that instrument and their normalization. We report on this reanalysis here and summarize the relevant steps below. With the result $B_\gamma=(3.8\pm0.4)\times10^{-5}$ the discrepancy is reduced but not completely removed.

## II. EXPERIMENTAL DETAILS

### A. Setup

In our experiment muons from the most intense muon beam at the Swiss Institute of Nuclear Research (SIN) were brought to rest in a 7-cm-thick, 13.3-cm-diam, thin plastic container filled with light water from the early part, and heavy water from the major part of the experiment. Apart from the target, the setup otherwise was completely identical to that used with the $^{40}Ca$ target.[5] During most of our run the average muon intensity was $6.2\times10^6$ sec$^{-1}$, but part of the data were taken in a period where the primary proton beam was pulsed with a frequency of 400 kHz. This beam structure was required for a rare muon conversion experiment.[7] The detailed time dependence of the beam intensity is given in this Ref. 7 (typically a nearly Gaussian pulse with FWHM 0.6 $\mu$sec and peak intensity $17\times10^6$ sec$^{-1}$ appearing every 2.5 $\mu$sec). During these periods we consequently divided our data into two nearly equal time gates, one overlapping the beam pulse, the other one covering the beam off

 

phase. During the latter gate still nearly half of the events occured, since the muon lifetime in $^{16}O$ [1.80 $\mu$sec (Ref. 8)] is still long enough, but the part of the photon spectrum induced by the pion- and electron-beam contamination was absent. Photons were detected in the Lausanne-München-Zürich pair spectrometer described in details elsewhere.[9] To shift the peak in the acceptance to lower energies we worked with a 0.6 T magnetic field and used a 600-$\mu$m Pb foil followed by a thin multiwire proportional chamber and a 176-$\mu$m Au foil to convert the photons. The chamber between the two converters allows to determine the origin of the pair. The details of the pattern recognition in the multiwire proportional chambers and the selection of genuine electron-positron pairs originating from a converter are described in Refs. 5 and 9. The calibration procedure with stopped poins in hydrogen and the details of the response function are given also in Ref. 5. The $^{16}O$ data presented here were bracketed by the early $^{40}Ca$ data, taken with two 88-$\mu$m Au converters and a later set taken in the configuration described above. In Fig. 1(f) the acceptance curve and resolution function for both converters is reproduced.

### B. Radiative muon capture spectrum and backgrounds

In Fig. 1 samples of different spectra are shown, which already indicate the principal source of background in this experiment. Since only 18.3% of all muons are captured by the nucleus, while the remainder decays in orbit, since furthermore the radiative pion capture branching ratio in $^{16}O$ is 2.2% (Ref. 10) or 580 times larger than the radiative muon capture branching ratio, we found about seven times as many $(\pi^-,\gamma)$ compared to $(\mu^-,\nu_\mu\gamma)$ photons in the energy region above the muon decay bremsstrahlung continuum endpoint, despite the fact that the pion contamination in the beam is only 0.12%. For the runs taken with unpulsed primary beam of $5.4\times10^6$ $sec^{-1}$ stopping muons in $D_2O$ which constitute 60% of our total event sample, we recorded $6.2\times10^6$ events in 144 h of data taking leading to $9.6\times10^4$ reconstructed photons, 1300 radiative muon capture, 9200 radiative pion capture, and 86 000 muon decay bremsstrahlung events, i.e., a rate of nine good events per hour was achieved.

Pion-induced events are tagged via a prompt 20- (in some runs 30-) nsec wide time gate opened by an arriving beam particle. The efficiency of this tagging method can be judged again from Fig. 1. In the energy region beyond the muon mass nearly all events are prompt. The content of the two spectra can be written ($N\equiv dN_\gamma/dE_\gamma$) as

$$\text{prompt: } N^{\text{pr}}=f_3N^\pi+f_1N^\mu ,$$

$$\text{nonprompt: } N^{\text{npr}}=(1-f_3)N^\pi+(1-f_1)N^\mu ,$$

$$N=N^\pi+N^\mu=N^{\text{pr}}+N^{\text{npr}} .$$

$f_3$ represents the efficiency of the prompt tag, typically 80–90% (see Table I), determined for $E_\gamma>90$ MeV, where $N^\mu=0$. $f_1$ represents the fraction of muon events appearing during the early part of the muon lifetime or together with random, second muons during the prompt gate. This factor varies between 0.03 (beam off, pulsed beam) and 0.25 (see Table I). Below 50-MeV photon energy nearly all events are due to muon decay electrons radiating due to interaction in the target and therefore $N^\pi \ll N^\mu$, which allows to determine $f_1$ in this region.

For each run period we construct four photon spectra, i.e., for each converter

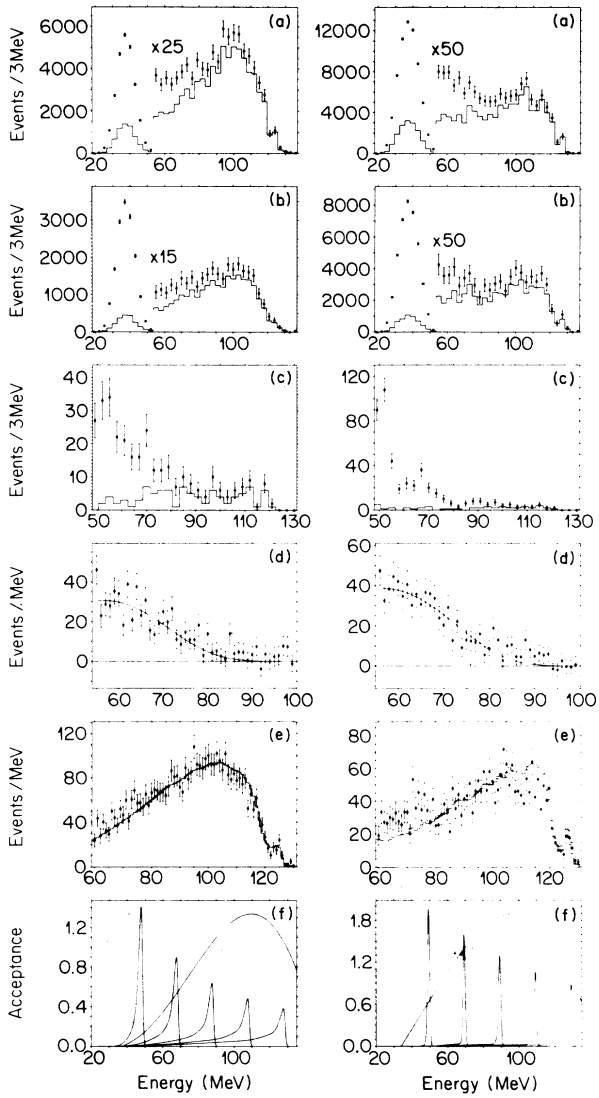


FIG. 1. Various photon spectra relevant to this experiment. Right: 176-$\mu$m Au converter; left: 600-$\mu$m Pb converter. (a)–(c) Raw photon spectra for the two different beam periods (3-MeV bin width). The data points with error bars indicate the full spectrum, the histogram represents the prompt contribution, coming mainly from the pion contamination in the beam. (a) Unpulsed beam, heavy-water target. (b) Pulsed beam, light- and heavy-water targets summed during beam pulse. (c) Pulsed beam, between beam pulses (note the near absence of the prompt contribution). (d) Spectrum of muon-induced events, target container not subtracted (1-MeV bin width). The solid line shows the folded theoretical prediction for $^{16}O(\mu,\nu_\mu\gamma)$ (Ref. 11). (e) Spectrum of pion- (and electron-) induced events (1-MeV bin width). The histogram shows the $^{16}O(\pi^-,\gamma)^{16}N$ (Ref. 10) spectrum folded with our acceptance and resolution. (f) Relative acceptance curve (normalized to 1 at 130 MeV) and typical resolution curves (area normalized to 1) for 50-, 70-, 90-, 110-, and 130-MeV photon energy deduced from pion calibration data with a hydrogen target (Ref. 5).

TABLE I. Consistency check for the different data sets. $f_3$—efficiency of prompt tag; $f_1$—fraction of muon events in prompt gate; $N^{\text{all}}$—total number of events in the energy region 56–89 MeV (Au converter) and 55–88 MeV (Pb converter); $N^{\text{pr}}$, $N^{\mu}$, and $N^{\pi}$—number of prompt, muon, and pion events in the same energy regions (see text). The "beam-off" sample is a subset of the pulsed beam data (see text). For all event samples a cut on the origin of the photon along the beam axis has been applied (see text); no target out subtraction has been made. $B(\mu^-,\nu_\mu\gamma)$—radiative muon-capture branching ratio for photon energies above 57 MeV computed from $N^{\mu}$ using appropriate normalization factors. The error includes only the statistical error from each data set, not the systematical error of the normalization factor, common to all sets. Corrections for target-out contributions and losses of good events in the cut are included in the normalization factors.

| Target (converter) | $\frac{f_1}{f_3}$ | $N^{\text{all}}$ | $N^{\text{pr}}$ | $N^{\pi}$ | $N^{\mu}$ | $B(\mu^-,\nu_\mu\gamma)\times 10^5$ |
|---|---|---|---|---|---|---|
| Unpulsed | | | | | | |
| $D_2O$ (Au) | 0.2481±0.0015 | 1174 | 675 | 604±32 | 570±32 | 4.09±0.23 |
| $D_2O$ (Pb) | 0.8824±0.0060 | 1359 | 965 | 990±39 | 369±29 | 3.89±0.31 |
| Pulsed | | | | | | |
| $H_2O$ (Au) | 0.0870±0.0018 | 418 | 238 | 285±21 | 133±17 | 3.06±0.38 |
| $H_2O$ (Pb) | 0.7950±0.0133 | 489 | 314 | 384±24 | 105±17 | 3.55±0.58 |
| $D_2O$ (Au) | 0.1655±0.0022 | 329 | 188 | 188±17 | 141±15 | 3.19±0.34 |
| $D_2O$ (Pb) | 0.8744±0.0116 | 436 | 285 | 301±21 | 135±16 | 4.46±0.52 |
| Beam off | | | | | | |
| $H_2O+D_2O$ (Au) | 0.028±0.012 | 149 | 11 | 10± 5 | 139±13 | 3.58±0.33 |
| $H_2O+D_2O$ (Pb) | 0.717±0.047 | 148 | 42 | 54±10 | 93±12 | 3.52±0.45 |
| All (Au) | 0.2012±0.0011 | 1921 | 1100 | 1077±42 | 844±39 | 3.72±0.18 |
| All (Pb) | 0.8638±0.0050 | 2282 | 1564 | 1667±58 | 615±38 | 3.98±0.24 |

$$N^{\pi}=[N^{\text{pr}}-f_1N]/(f_3-f_1)\ ,$$

$$N^{\mu}=[N^{\text{npr}}-(1-f_3)N]/(f_3-f_1)\ .$$

The pion spectra [Fig 1(e)] are well represented by the folded $^{16}O(\pi^-,\gamma)^{16}N$ spectrum of Strassner *et al.*[10] In the low-energy region between 50 and 80 MeV there is a small excess of events in these spectra, which we ascribe to wide-angle bremsstrahlung from the electron contamination in the beam. In fact with 1% contamination[12] we expect about 50 events each in the $\mu$-capture region of these spectra based on an electron photon shower Monte Carlo simulation (EGS) (Ref. 13) with 115 MeV/$c$ electrons colliding with a 22% radiation length water target. In the spectra taken during the "beam-off" gate in the pulsed beam mode [Fig. 1(c)] the prompt background is nearly absent, apart from a few events induced by the tails of the beam pulse. The muon-induced events [Fig. 1(d)] follow the predicted theoretical shape folded with the spectrometer response function.

From the electron and positron momentum vectors the photon direction and its intersection with a vertical plane containing the beam line can be reconstructed. In our previous experiment[5] with a thinner converter we used a cut on this quantity to reject nearly all nontarget associated photons. The multiple scattering in the thicker converter foils employed here leads to a deterioration of the resolution and consequently to a large loss of good events, too, as Fig. 2 demonstrates. We therefore subtracted the target empty spectra normalizing to the number of incoming muons for the final spectra shown in Fig. 3. The overall target empty contribution is only 3.2%, but in the $\mu$-capture region it is 10% for muon- and 32% for pion-induced events, since the muon decay bremsstrahlung is suppressed for the empty container.

The average energy loss of the electron positron pair in the Pb converter is 6.4 MeV and 1.8 MeV in the Au converter. With EGS-shower code simulations[13] of the bremsstrahlung spectrum (see also Refs. 1 and 5) we established that the measured (unshifted) energy regions above $E_{\text{min}}=55$ MeV (Pb) and $E_{\text{min}}=56$ MeV (Au) are free from this background, even considering tails of the resolution function. The maximum photon energy for $^{16}O(\mu^-,\nu_\mu\gamma)^{16}N$ (ground state) is $E_0=94.3$ MeV, but due to the phase-space factor $1-(E_\gamma/E_0)^2$ the yield above 90 MeV is essentially zero. From these considerations we selected for fits and consistency checks between different data subsets the regions 55 to 88 MeV (Pb) and 56 to 89 MeV (Au), respectively, and treated always both converters separately, apart from the final, unfolded spectrum of Fig. 3(c).

### C. Normalization and results

The background subtracted spectra were fit to the following expressions:

$$\frac{dN_\gamma^\mu}{dE_\gamma}=B_\gamma N_0\int B(E)A_{\text{rel}}(E)R(E,E_\gamma)dE$$

in the region $E_{\text{min}}<E_\gamma<E_{\text{max}}$. $B(E)$ is given by the theoretically predicted differential photon spectrum, normalized such that

$$\int_{57\text{ MeV}}^{E_0}B(E)dE=1\ ,$$

$$B(E)=\frac{1}{B_\gamma^{\text{theory}}}\frac{1}{\Lambda(\mu^-,\text{all})}\frac{d\Lambda_\gamma^\mu(E_\gamma)}{dE_\gamma}\ .$$

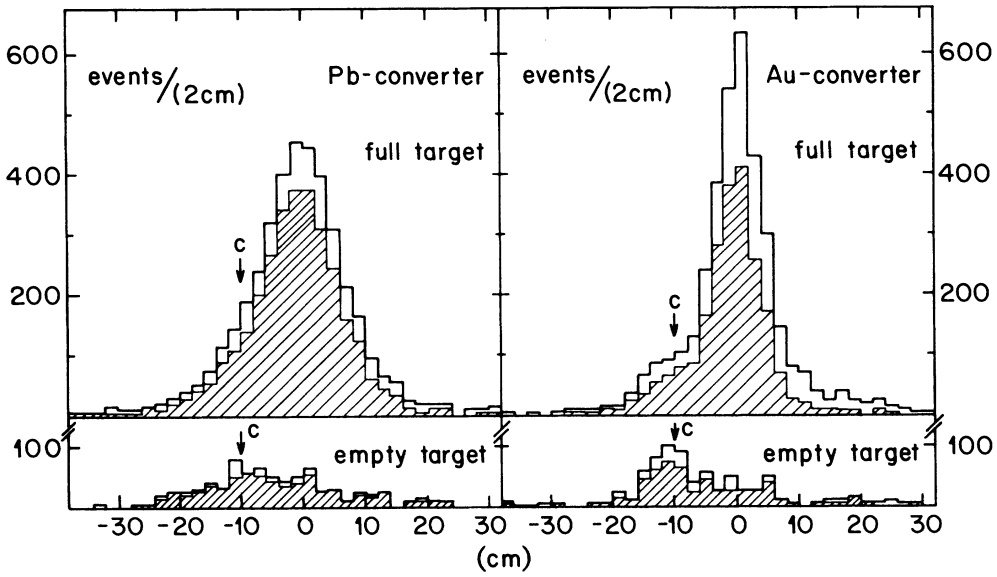


FIG. 2. Reconstructed origin of photons with energy exceeding 50 MeV along the beam axis measured relative to the target center. The arrow marks the end of the degrader (and last beam defining counter) and the position of the target cut used for the data of Table I. The target width is 7.7 cm in beam direction. The data are from the unpulsed beam period with a $D_2O$ target. The shaded areas indicate the prompt part of the events.

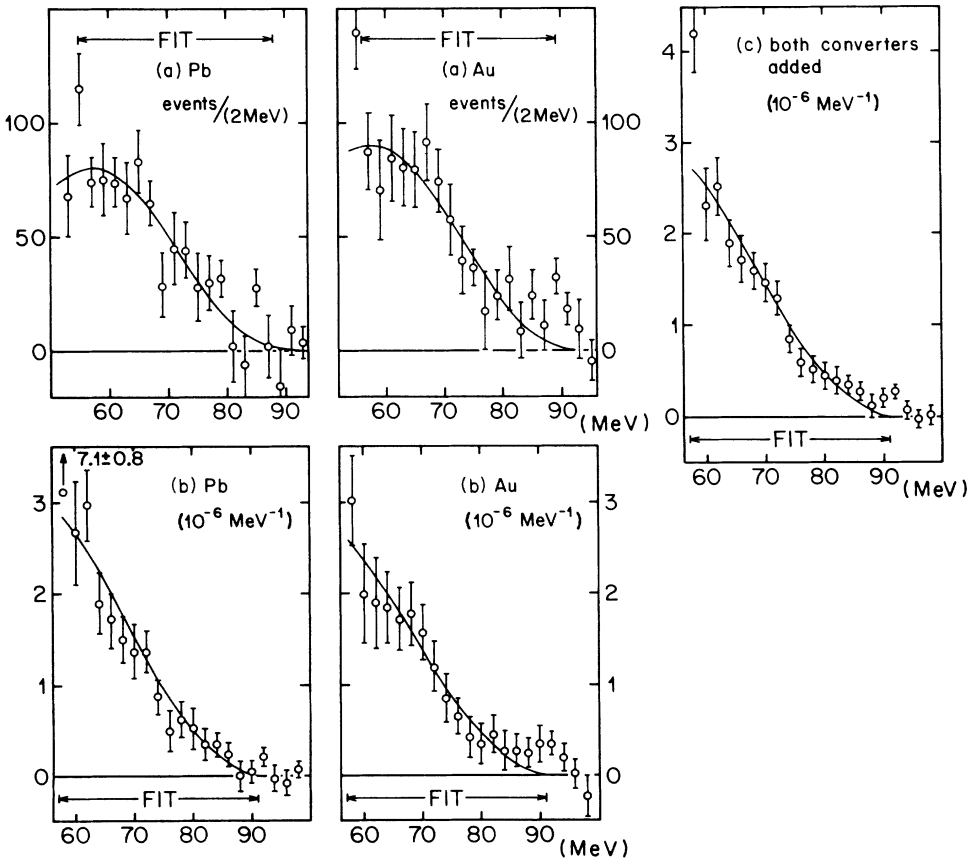


FIG. 3. (a) Final radiative muon-capture spectra with target empty background subtracted for both converters compared to the folded theoretical spectra [best-fit results (Ref. 11)]. (b) and (c) unfolded and normalized radiative muon-capture spectra. All run periods (b) and both converters (c) were added after shifting the Au converter data upwards in energy by 1.8 MeV and the Pb converter data by 6.4 MeV and dividing out the energy-dependent detector efficiency. The solid curves represent the best-fit theoretical prediction (Ref. 11).

We used the theory of Christillin and Gmitro[11] with the standard value of $g_P/g_A=6.8$ for $B(E)$ in our fits. The value of $g_P$ influences the shape of $B(E)$ very little. Consequently the free parameter for the fit $B_\gamma$ does not depend on this particular choice for $g_P$. With $B_\gamma$ we directly obtain the desired integrated yield above 57 MeV, which all previous experiments[2] quote, provided that the normalization parameter $N_0$ is properly chosen (see below). $B_\gamma$ can then be compared to $B_\gamma^{\text{theory}}$, the integrated theoretical yield, which depends strongly on $g_P$. $R(E,E_\gamma)$ is the normalized resolution function and $A_{\text{rel}}(E)$ the relative acceptance of the spectrometer. The absolute acceptance $A_0$ at 130 MeV is contained in $N_0$, which can be written as

$$N_0=\mu_{\text{in}}\times f_{\text{stop}}\times f_{\text{cap}}\times(1-f_{\text{abs}})\times A_0 ,$$

$$A_0=(5.92\pm0.21)\times10^{-5}\ \text{(Pb) (Ref. 5)}=(2.44)\pm0.10)\times10^{-5}\ \text{(Au) (Ref. 5)} ,$$

$\mu$ = number of incoming muons $=5.3\times10^{12}$ for the full data set ,

$f_{\text{stop}}=0.87\pm0.02$ = fraction of muons stopping in the target ,

$f_{\text{cap}}=1-\tau_\mu(^{16}\text{O})/\tau_\mu(\text{free})=0.183\pm0.001$ (Ref. 8)

= fraction of muons captured by the nucleus ,

$f_{\text{abs}}=0.12\pm0.02$ = fraction of photons absorbed in the target .

The number of muons $\mu$ has been corrected for counting losses and counter inefficiencies. At $6.2\times10^6$ sec$^{-1}$ beam intensity, where most of our data were taken, this correction is $23\pm7$ %. It was determined from the rate dependence of the photon yield (a low statistics run at 0.3, the majority of the runs at 6.2, and the pulsed runs at peak intensity $17\times10^6$ sec$^{-1}$) and three special runs recording the positive muon decay bremsstrahlung spectrum at 2.7, 16, and $23\times10^6$ sec$^{-1}$ beam intensity. The uncertainties in the parameters of the relative acceptance function[5] contribute $\pm4.6$% relative error. Summing all independent contributions in quadrature gave a total systematic normalization error of 9%. The latter includes also $\pm2.5$% from the $\pm200$-keV uncertainty in the absolute energy scale.[5]

Using the fact that

$$\int_{E_{\text{min}}}^{E_{\text{max}}}\frac{dN_\gamma^\mu}{dE_\gamma}dE_\gamma=\beta B_\gamma ,$$

with $\beta=0.413$ (Pb) and $\beta=1.242$ (Au), we may simply sum all events between $E_{\text{min}}$ and $E_{\text{max}}$ and divide by $\beta N_0$ to obtain an estimate of the integrated yield for the different data sets. This was done for the data summarized in Table I. To avoid the contribution of target-out subtraction to the statistical error, we used for this consistency check data with a target cut (see Fig. 2). This implies a 15% upward correction for the Pb converter data to account for the excess of good events lost in the cut, while for the Au converter the latter balance with the target-out background kept in the spectrum. There is no significant trend visible in these results. Independent of the respective pion-to-muon ratios, the beam periods or the converter type, the results are consistent with the average values within their statistical errors.

The fit to the summed and background subtracted spectra of Fig. 3(a) yields

$$B_\gamma=(3.90\pm0.24)\times10^{-5}\ \text{(Pb)} ,$$

$$B_\gamma=(3.60\pm0.25)\times10^{-5}\ \text{(Au)} ,$$

respectively, for the integrated theoretical curve and

$$B_\gamma=(3.97\pm0.33)\times10^{-5}\ \text{(Pb)} ,$$

$$B_\gamma=(3.72\pm0.29)\times10^{-5}\ \text{(Au)} ,$$

respectively, from summing the data as done for Table I.

For the final result we average the two statistically independent results for the two converters to obtain

$$B_\gamma=\Lambda(\mu^-,\nu_\mu\gamma;E_\gamma>57\ \text{MeV})/\Lambda(\mu^-,\text{all})$$
$$=(3.8\pm0.2)\times10^{-5}\ \text{(statistical)}$$
$$=(3.8\pm0.4)\times10^{-5}$$
(including systematic errors) .

As in our previous pairspectrometer experiment on $^{40}$Ca we also deduce unfolded spectra by shifting the spectra by the average energy loss and dividing by the normalization constant and the relative acceptance. The results are shown for both converters individually in Fig. 3(b) and summed in Fig. 3(c). A fit to the latter spectra yields an average value $B_\gamma=(3.9\pm0.2)\times10^{-5}$ (statistical) again consistent with the above result. However this procedure is only approximately correct and is done solely to facilitate the comparison with future theoretical calculations. In particular the first bin of the Pb-converter spectrum can be seen to be already affected by tails of the bremsstrahlung spectrum feeding into the muon-capture region because of the broader resolution function. To obtain the differential radiative muon-capture rate the data of Table II should be multiplied by $\Lambda(\mu^-,\text{all})-102\,300\pm600$ sec$^{-1}$.[8]

TABLE II. Differential photon spectrum for $^{16}O(\mu^-,\nu_\mu\gamma)$ with resolution and acceptance unfolded. A ±9% uncertainty in the overall normalization is not included in the errors given for the individual ponts. The energy refers to the center of the 2-MeV bin.

| Energy (MeV) | $dN_\gamma/dE_\gamma\times10^6$ (MeV$^{-1}$) | Energy (MeV) | $dN_\gamma/dE_\gamma\times10^6$ (MeV$^{-1}$) | Energy (MeV) | $dN_\gamma/dE_\gamma\times10^6$ (MeV$^{-1}$) |
|---|---|---|---|---|---|
| 58 | 4.20±0.42 | 72 | 1.30±0.17 | 86 | 0.27±0.10 |
| 60 | 2.32±0.39 | 74 | 0.86±0.16 | 88 | 0.13±0.12 |
| 62 | 2.53±0.31 | 76 | 0.60±0.15 | 90 | 0.19±0.09 |
| 64 | 1.89±0.25 | 78 | 0.53±0.15 | 92 | 0.27±0.07 |
| 66 | 1.72±0.24 | 80 | 0.45±0.14 | 94 | 0.07±0.11 |
| 68 | 1.60±0.21 | 82 | 0.40±0.13 | 96 | −0.03±0.11 |
| 70 | 1.48±0.21 | 84 | 0.34±0.11 | 98 | 0.02±0.09 |

## III. DISCUSSION

Using the model of Gmitro and Christillin[11] our experimental value for $B_\gamma$ corresponds to a value of $g_P/g_A=13.5\pm1.5$. We determine the value and its error by linear interpolation of the two values given in Ref. 11, namely $B_\gamma^{\text{theory}}=2.08\times10^{-5}$ for $g_P/g_A=6.8$ and $B_\gamma^{\text{theory}}=3.84\times10^{-5}$ for $g_P/g_A=13.6$, respectively. If we take the weighted average of our present and the NaI data,[1] $B_\gamma=(3.3\pm0.6)\times10^{-5}$ (increasing the error because the two data sets disagree by two combined standard deviations), we would obtain $g_P/g_A=11.8\pm2.4$, as shown in Fig. 4. This result is consistent with the analysis of muon capture [$^{16}O(\mu^-,\nu_\mu\gamma)^{16}$ N$(0^-)$] and $\beta$ decay [$^{16}$N$(0^-)(e^-\bar{\nu}_e)^{16}$O] involving the lowest $0^-$ state in $^{16}$N,[14] which gave $g_P/g_A\approx12.5$. It is furthermore consistent with the only other measurement in a light system from $^{12}C(\mu^-,\nu_\mu)^{12}$B (ground state) polarization quantities, which gave $g_P/g_A=9.0\pm1.5$.[15] The reasons why all these measurements seem to imply an enhancement of the pseudoscalar coupling in light nuclear systems are, however, not clear.

The combination of our present data and those of Ref. 1 have furthermore resolved the major discrepancy between experiment and theory discussed in detail in the review of Gmitro and Truöl.[2] $^{16}$O is a particularly attractive model case, since the wave functions used in the calculations[11,16,17] has been well tested against data from other weak and electromagnetic processes, e.g., inelastic electron scattering and radiative pion capture. The nuclear response is dominated by spin-isospin states $J^\pi=0^-,1^-,2^-$, with the $T=1$ magnetic quadrupole states being most important. Their structure is primarily of $|1d_{5/2}1p^{-1}_{3/2,1/2}\rangle$ nature with strong $2p2h$ admixtures. With these configurations it was shown that the modified impulse approximation (MIA) calculations,[16] where current conservation was imposed at the electromagnetic vertices via Siegert's theorem, lead to a considerable reduction of the predicted rate compared to the standard impulse approximation (IA) results, using the same wave functions.[17] The results brought the calculations into agreement with the phenomenological ansatz used by Gmitro and Christillin,[11] which we referred to above. In the latter calculation the nuclear response is split into the $^{16}$N bound-state quartet ($0^-$ to $3^-$) and a dipole part, as-

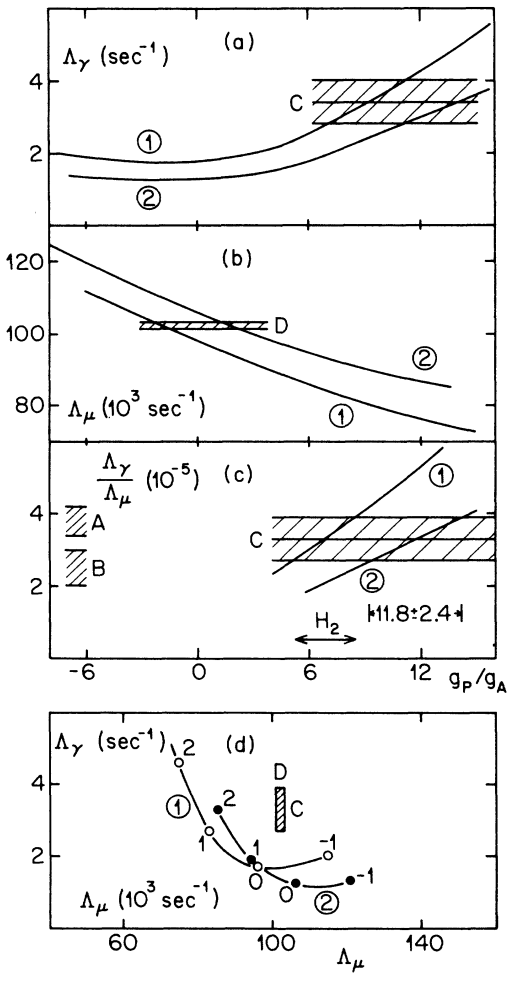


FIG. 4. (a)–(c) influence of the induced pseudoscalar coupling constant $g_P$ on the radiative ($\Lambda_\gamma$) and ordinary ($\Lambda_\mu$) muon-capture rate in $^{16}$O. The nucleonic value is indicated, too. (1) Shell-model and standard impulse approximation (IA) (Ref. 17). (2) Modified impulse approximation (MIA) with shell-model (Ref. 16) and/or phenomenological response function (Ref. 11). *A*, data of Ref. 1; *B*, this experiment; *C* average of *A* and *B*; *D*, Ref. 8. (d) $\Lambda_\gamma$ vs $\Lambda_\mu$. The points labeled −1, 0, 1, and 2 refer to $g_P/g_A$ in units of the standard value $g_P/g_A=6.8$.

suming degeneracy of the isospin giant-dipole photonuclear resonance and the spin-isospin levels mentioned above, and measured form factors for these structures are used to obtain predictions. With the higher, preliminary radiative capture rates at the time of the review[2] the whole approach needed to be questioned. This is now no longer necessary. However, it is clear that further fine tuning of the calculations is required, because as evident from Fig. 4, no calculation can reproduce the ordinary muon-capture rate $\Lambda_\mu$ and the radiative muon-capture rate $\Lambda_\gamma$ at the same time. The ratio of these two quantities, which vary with $g_P$ in opposite directions, is however believed to be less model dependent, if both rates are computed within the same frame.

## ACKNOWLEDGMENTS

We thank Dr. W. Dahme, Dr. R. Kopp, and Professor W. Hering, all from Universität München, for their assistance during the data taking, Professor C. Zupančič, Universität Müchen for his continued support of this experiment, and Dr. M. Gmitro, JINR Dubna for numerous helpful discussions concerning the radiative muon-capture calculations. The experiment was further strongly supported by Professor J. P. Blaser and his SIN crew, and the Swiss and German funding agencies for basic research, "Schweizerischer Nationalfonds" and "Deutsche Forschungsgemeinschaft."

---

*Present address: Volpi AG, CH-8952 Schlieren, Switzerland.
†Present address: Physics Department, CALTECH, Pasadena, California 91125.
‡Present address: Institut für Astronomie, ETH, CH-8092 Zürich, Switzerland.
§Present address: IABG, D-8012 Ottobrunn, Germany.
**Present address: NAGRA, CH-8401 Baden, Switzerland.
††Present address: BMW AG, D-8000 München 40, Germany.

[1]M. Döbeli *et al.*, Phys. Rev. C **37**, 1633 (1988).
[2]M. Gmitro and P. Truöl, in *Advances in Nuclear Physics,* edited by J. W. Negele and Erich Vogt (Plenum, New York, 1987), Vol. 18, p. 241.
[3]G. Bardin *et al.*, Nucl. Phys. **A352**, 365 (1981).
[4]R. D. Hart *et al.*, Phys. Rev. Lett. **39**, 399 (1977).
[5]A. Frischknecht *et al.*, Phys. Rev. C **32**, 1506 (1985).
[6]A. Frischknecht *et al.*, Proceedings of the International Symposium on Mesons and Light Nuclei, Liblice, Czechoslovakia, 1981 [Czech. J. Phys. B **32**, 270 (1982)].
[7]A. Badertscher *et al.*, Nucl. Phys. **A377**, 406 (1982).
[8]M. Eckhause, R. T. Siegel, and R. E. Welsh, Nucl. Phys. **81**, 575 (1966); T. Suzuki, D. F. Measday, and J. P. Roalsvig, Phys. Rev. C **35**, 2212 (1987).
[9]J. C. Alder *et al.*, Nucl. Instrum. Methods **160**, 93 (1979).
[10]G. Strassner *et al.*, Phys. Rev. C **20**, 248 (1979).
[11]P. Christillin and M. Gmitro, Phys. Lett. **150B**, 50 (1985).
[12]Swiss Institute of Nuclear Research Users Handbook, 1981 (unpublished), p. 37.
[13]R. L. Ford and W. R. Nelson, SLAC Report No. 210, UC-32, 1978 (unpublished).
[14]A. R. Heath and G. T. Garvey, Phys. Rev. C **31**, 2190 (1985).
[15]L. Ph. Roesch, V. L. Telegdi, P. Truttmann, A. Zehnder, L. Grenacs, and L. Palffy, Helv. Phys. Acta **55**, 74 (1982).
[16]M. Gmitro, A. A. Ovchinnikova, and T. V. Tetereva Nucl. Phys. **A453**, 685 (1986).
[17]M. Gmitro, S. S. Kamalov, T. V. Moskalenko, and R. A. Eramzhyan, Czech. J. Phys. B **31**, 499 (1981).